Effect of carbonization temperature on properties of char from coconut shell

U. F. Hassan [1] , A. A. Sallau1[1,4*], E. O. Ekanem [2], A. Jauro [3], A. M. Kolo [1]

[1] *Chemistry department, Abubakar Tafawa Balewa University Bauchi, Bauchi State*
[2] *Chemistry department, Federal University Otuoke, Bayelsa State*
[3] *National Environmental Standards and Regulations Enforcement Agency (NESREA), Abuja*
[4] *Sheda Science and Technology Complex, Abuja*
Corresponding author E-mail: creamysal@yahoo.co.uk

Abstract

The study Investigate the effect of carbonization temperature on properties of coconut shell. The carbonization was carried out at 600, 800, 1000 and 1150°C temperatures for 1 hour under inert condition. The derived chars were proximately, ultimately and structurally analyzed. The results show that there was a significant change in the volatile matter, fixed carbon percentage, elemental C and its functional group as temperature increases. The moisture content and percentage yield decrease with increasing temperature. The morphological characterization of the materials shows fibrous nature of the raw samples while the char products show developed pores which are suitable for adsorption, movement of electrolyte ions and reduced diffusion resistance. The electrical properties of char improved from 3.52×10^{-8} to 6.78×10^{-2} S/cm as temperature increases from 600°C to 1150°C. results from X-ray diffractometer analysis showed improved graphitic properties; which suggest a possible use of the char samples particular the PKS1150 in electrode fabrication material.

Keywords: *Biomass; Carbonization; Correlation; Morphology; Stacking.*

1. Introduction

Coconut (Cocos Nucifera) is a member of the Acecacaae (palm) family. It a large palm tree, growing up to 30m tall, with pinnate leaves of 4-16m long and 60-90cm in diameter (Li et al., 2008; Ewansiha et al., 2012; Iloabachie et al., 2018). The term coconut can refer to the entire coconut palm, the seed, or the fruit, which is not a botanical nut. The fully developed hard shell which houses the nut does not crack easily, Ewansiha et al (2012). The shell of the coconut is one part of the waste after removing the husk, which is a very hard lignocellulosic material that can be converted to carbon black through carbonization (Ojha et al., 2016). Such carbon black material may be adapted for use as gas absorber, water purifier and as catalyst in electrical conducting materials (Lee et al., 2017).

The coconut shells have been the subject of many investigations for the production of activated carbons (Olowolo and Orere,2012; Tangsathitkulchai et al., 2013; Sulistyani et al., 2015) while some other studies focused on its suitability for its use in composites (Ojha et al., 2016), and as nanocrystalline graphite (Wachid et al.,2014). The optimization of the use of these shells in the composites requires the knowledge of its physical, chemical and mechanical properties (Njeugna et al., 2013). The current study, hopes to carbonize coconut shell powder at varying temperature from 600 to 1150°C, characterize the carbon char obtained for its proximate, ultimate, structural, morphological, crystalline and electrical properties for possible use in electrode material formulation.

2. Experimental

Coconut shell was purchased from Gwagwalada market, F.C.T., Abuja, Nigeria. The shells were air dried for 48 hours, grinded and sieved with 2mm sieve. These were then packed into a stainless steel combustion tube (410mm long, 34.5mm inner and 42.5mm outer diameter) and placed in thermolyte tubular furnace then heated at 600°C, 800°C, 1000°C and 1150°C temperatures under nitrogen gas atmosphere for 60mins. The coconut shell particles and char products were characterized using standard methods of American Society for Testing and Materials (ASTM) method D 4442 – 07 and D1762-84 for the proximate analysis, Perkin Elmer's 2400 Series II CHN Elemental Analyzer was used for ultimate analysis, the morphological structure was studied using Phenom ProX scanning electron microscope at central laboratory of the Umar Musa Yar'adua University, Katsina, Nigeria. Functional group was investigated using Thermo Scientific Nicolet iS5 FT-IR Spectrometer at Chemistry Advanced Research Center, Sheda Science and Technology Complex (SHESTCO), Abuja, Nigeria. Crystal structure by Empyrean (panalytical) diffractometer (at National geological research laboratory, Kaduna, Nigeria). While the electrical properties were investigated using four-point probe, attached to a Keithley source meter for voltage, current sourcing and a computer

with labtracer 2.0 software for data display. Data obtained from FTIR and XRD study were further subjected to principal component analysis (PCA).

3. Result and discussions

3.1. Proximate analysis and ultimate analysis

The result from the proximate investigation displayed in Table 1, showed that the raw CNS had high volatile matter of 73.12 %, a fixed carbon of 19.59%, and ash content of 1.98%. While the moisture content of the raw sample was 5.31%. The yield of CNS char was found to reduces from 28.51% to 25.70% as the temperature increases from 600 to 1150°C. This is possibly due to the fact that increasing temperature forced some of the volatile components of the CNS to be lost (Abugu et al., 2014). The effect of change in temperature on the char yield, indicates that the lower yield obtained at 1150°C is caused by a much larger release of volatile matters, thus giving a lower content of volatile matters in the derived CNS1150 char. It can also be seen that higher carbonization temperature resulted in a higher fixed carbon content char as compared to lower carbonization temperature. This may suggest that the char obtained at higher temperature are most stable than those obtained at lower temperature (Lee et al., 2017). Similarly; the results from the elemental composition showed that the percentage carbon increase significantly in all the char obtained at different temperatures. The elemental carbon percent increase from 49.795 in CNS raw to 88.69% for CNS 600, while CNS1150 elemental carbon increase to 98.66%. The electrical resistivity and conductivity values for char obtained increases as the treatment temperature increase. This may suggest that temperature, heating condition and time have profound influence on the properties of char obtained.

Table 1: Proximate and Ultimate Analysis Carbon Material and Char Products

	proximate				Ultimate					Resistivity	Conductivity
	Yield	MC	VM	FC	Ash	C	H	O	N	S	ρ (Ω*cm)	S/cm
CNS Raw		5.31	73.12	19.59	1.98	49.79	6.22	42.24	1.61	0.14	-	-
CNS600	28.51	2.47	10.44	85.05	2.04	88.69	4.41	6.67	0.21	0.02	2.84×10^7	3.52×10^{-8}
CNS800	25.66	1.89	8.35	87.64	2.12	92.12	2.02	5.74	0.11	0.01	198.80	5.03×10^{-3}
CNS1000	25.11	1.27	3.06	93.26	2.41	97.59	0.81	1.52	0.07	0.01	41.61	2.40×10^{-2}
CNS1150	25.7	0.13	2.15	95.26	2.46	98.66	0.12	0.12	0.09	0.01	14.76	6.78×10^{-2}

Key: MC-Moisture content, VM- volatile matter, FC-fixed carbon

3.2 Electrical resistance and conductivity

Electrical conductivity (EC) is considered a fundamental property of a conducting material which indicates its ability to allow flow of electric current (Bogeat, 2019). The EC of carbon materials is directly related to their carbon content, especially the poly-aromatic carbon content. The poly-aromatic carbon in carbonized biomass are usually organized as random sheets of graphene, which are directly influenced by the temperature and reaction time of the carbonization process (Hoffmann et al., 2019). The electrical conductivity of a 20mm x 4mm circular disc of CNS char compressed with a force of 10N, increased from 3.52 x 10^{-8} S/cm at 600°C to 6.78 x 10^{-2} S/cm at 1150°C. Even though compression force has been shown to influence improved electrical conductivity in bio-carbon materials (Mochidzuki et al.,2003; Bogeat, 2019; Hoffmann et al., 2019), the main factor responsible for the improve electrical conductivity is suggested to be the heat treatment. Other factors such as crystallinity, activation, presence of pores have been reported to influence the electrical conductivity as well (Huggins et al., 2014). Thus it is evident that the increase carbonization temperatures led to increased amount of conductive phase in the carbonized PKS by incorporating more carbon atoms into the turbostratic crystallites of the char to form large graphene sheets (Kwon et al., 2013).

3.3. FTIR analysis

The FTIR spectra obtained for the raw CNS and char products at different carbonization temperatures is shown in Fig 1. The CNS raw showed broad band peak at 3303.83 cm^{-1} which is suspected to be due to O-H group, tiny peaks at 2924.82cm^{-1} is due to C-H stretching vibration while that at 1737.11 cm^{-1} is due to unconjugated C=O possibly due to uronic anhydride and the 1216.84 cm^{-1} peak represents the C-O stretching in C-O-H of phenolic group (Liyanage and Pieris, 2015). The absorption peak at 1599.02 cm^{-1} represent stretching vibration of the C=C bond in the benzene ring skeleton (Ma et al., 2014). While the broad peak observed at 1057 cm^{-1} was due to the stretching mode of vibration of C–O of cellulose, hemicelluloses and lignin (Liu et al., 2015; Satheesh et al., 2019). The most observed absorption band in the CNS char samples were the peak at 1737.11, 1365.78, 1228.82 and 528.08 cm^{-1} positions. The C=O stretching vibration was observed at 1737.11 cm^{-1} which is attributed to ketone or carboxylic acid functional group, while 1228.82 cm^{-1} represent C-O stretching as suggested in CNS raw sample. There were weak peaks observed at 2969.82 cm^{-1} and 2360.17 cm^{-1} which are characteristic of C-H bond stretching of CH_2 groups and C-C stretching vibration found in the structure of carbon black (Rampe et la., 2011).
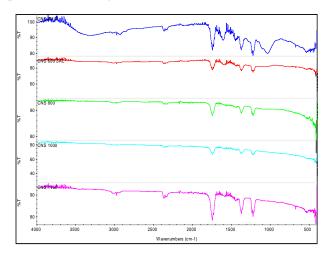
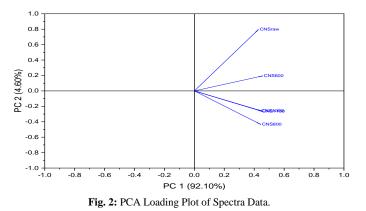**Fig. 1:** FTIR Spectra Plots of CNS Raw and Char Obtained at Different Temperature.

The raw data of the FTIR spectra were subjected to principal component analysis (PCA), to identify any differences between the structure of char samples as the temperature changes. It is common knowledge that PCA is often used reduced variable (Sanguansat, 2012; Liu et al., 2015). In PCA analysis, the samples that seemed alike usually are group together while those far to each other indicate their differences. This pattern of analysis provides clear discrimination between samples as a tool of identification (Noh et al., 2017).

Table 2: Result of Correlation Coefficient of CNS Spectra Data

	CNSraw	CNS600	CNS800	CNS1000	CNS1150
CNSraw	1	0.927	0.80649	0.84008	0.84862
CNS600	0.927	1	0.91665	0.9168	0.94863
CNS800	0.80649	0.91665	1	0.90879	0.94244
CNS1000	0.84008	0.9168	0.90879	1	0.95133
CNS1150	0.84862	0.94863	0.94244	0.95133	1

From the PCA results obtained, it was observed that the five samples were linearly correlated as shown in Table 2 with the correlation coefficient values been in the range of +0.8065 to +0.9513, hence the suitability of subjecting the samples to PC analysis. The Eigenvalues of the Correlation Matrix displayed in Table 3, showed the first principal components explaining 92.10% of the variance while the second principal components contributed only 4.60% and the rest each contribute less than 2% of the total variation.

Table 3: Eigenvalue of Correlation Matrix

	Eigenvalue	Percentage of Variance	Cumulative
1	4.60508	92.10%	92.10%
2	0.22995	4.60%	96.70%
3	0.0912	1.82%	98.52%
4	0.04673	0.93%	99.46%
5	0.02705	0.54%	100.00%

In addition, the PC loading plot of Fig. 2. Revealed the CNS-raw well separated and dissimilar to the char products even though both the raw and char samples were accounted for by only the PC 1. This reveals that the samples could be distinguished at some degree by the magnitude of carbonization temperature (Reeves, 2012).

Fig. 2: PCA Loading Plot of Spectra Data.

3.4. XRD analysis

The XRD spectra of CNS and its char at different carbonization temperatures are shown in Fig. 3. The diffractograms appeared to exhibit similar peaks (002) between 20-25, 2θ angle and peak (100) located between 42-47 2θ angle as the treatment temperature increases. These peaks are commonly attributed to the stacking of the graphitic basal plans of char crystallites (Wang et al., 2018). XRD theory has shown that asymmetric XRD peaks can be found when a sample has a stacked crystal structure or when the sample composition is not uniform. Thus a carbon material having a graphite structure shows asymmetry of the (002) peak due to stacking defects (Kang et al., 2018).
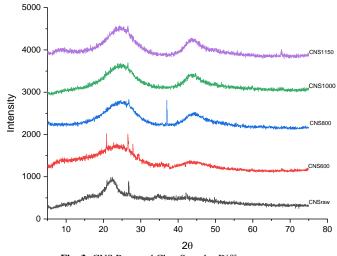
Fig. 3: CNS Raw and Char Samples Diffractograms.

Crystallite geometry in carbon materials parameters such as aromatic layer stacking height (Lc), diameter (La) and inter-layer spacing (d_{002}) are commonly estimated using the Bragg's law and Scherrer equation (Girgis et al., 2007; Stein et al., 2017).

$$d = \frac{\lambda}{2\sin\theta(002)} \tag{1}$$

$$L_c = \frac{0.94\lambda}{\beta(002)\cos\theta(002)} \tag{2}$$

$$L_a = \frac{1.84\lambda}{\beta_{100}\cos(\theta_{100})} \tag{3}$$

$$n\lambda = 2d_{002}\sin(\theta_{002}) \tag{4}$$

Where λ is the wavelength of the X-ray radiation, $d_{(002)}$ is the width of the (002) peak at half maximum of reflection, and θ is the Bragg peak position. Table 4, shows that, as carbonization temperature increases, the value of $d_{(002)}$ decreases from 3.9640 in the raw CNS to 3.6162 Å in CNS1150, whereas that of $d_{(100)}$ though absent in raw CNS, it increases fractionally from 2.0578 in the CNS600 to 2.0673 Å in CNS1150. It was observed that, the numerical variance of $d_{(002)}$ is greater than that of $d_{(100)}$, which is similar to the results of common carbon materials (Ma et al., 2014; Barnakov et al., 2015). Also it was noticed that the narrow peak at around 26-27 2theta disappeared as the carbonization temperature increased.

Table 4: Structure Parameters of X-Ray Diffraction for CNS Raw and Char Samples at Various Temperature

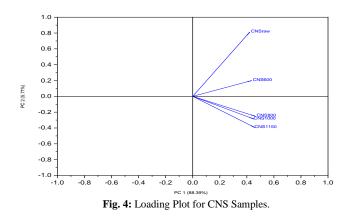| sample	d_{002} (A°)	d_{100}(A°)	L_c (A°)	L_c/d_{002}
CNS Raw	3.9640	-	0.100265	0.024671
CNS 600	3.3524	2.0578	0.671179	0.200173
CNS 800	3.6556	2.0638	0.338853	0.100933
CNS 1000	3.6044	2.0675	0.536687	0.159947
CNS 1150	3.6162	2.0673	0.046485	0.012745

PC analysis was performed on the XRD diffractograms data to detect similarities or difference in the CNS char samples obtained. The result indicated the sample data are highly correlated with all values greater than +0.5. Table 5, showed the details of the strength of linear relationships between the CNS raw and char samples. CNS1150 char sample was observed to show highest linear relationship of 0.9621 with CNS800.

Table 5: Correlation of CNS Diffractograms Data

	CNSraw	CNS600	CNS800	CNS1000	CNS1150
CNSraw	1	0.79362	0.80952	0.80979	0.76377
CNS600	0.79362	1	0.87203	0.77726	0.86971
CNS800	0.80952	0.87203	1	0.94319	0.96211
CNS1000	0.80979	0.77726	0.94319	1	0.93436
CNS1150	0.76377	0.86971	0.96211	0.93436	1

The Eigenvalues of the Correlation Matrix displayed in Table 6, shows the first principal components explaining 88.39 % of the variance while the second component explains 5.71 %. The third contribute 4.50% of the total variation.

Table 6: Eigenvalue of Correlation Matrix of Sample PCA

	Eigenvalue	Percentage of Variance	Cumulative
1	4.41956	88.39%	88.39%
2	0.28525	5.71%	94.10%
3	0.22516	4.50%	98.60%
4	0.03627	0.73%	99.32%
5	0.03376	0.68%	100.00%

While the PC loading plot displayed in Fig. 4. Showed the CNS800, CNS1000 and CNS1150 as group of similar variation.

Fig. 4: Loading Plot for CNS Samples.

3.5. SEM analysis

Scanning electron micrographs for external morphology of coconut shell powder and char obtained at temperatures 600℃, 800℃, 1000°C and 1150℃ are shown in Fig. 6. The raw CNS at 2000x magnification, showed stack of parallel solid flakes with relatively smooth surfaces with narrow pore path. The rise in carbonization temperature causes substantial transformation to the surface morphology of the chars as there was increase in the surface roughness, this is probably caused by the increased rupture of the biomass structure due to release of more volatile matter as the heating temperature was increased (Tangsathitkulchai *et al.,* 2016). Hence there were noticeable pore development on the surface of the chars. The presence of pores on the surface of PKS char are regarded as conducive to the movement of electrolyte ions and reduced diffusion resistance (Ding *et al.,* 2020).
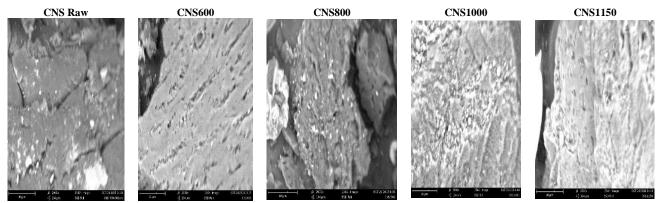

Fig. 5: Scanning Electron Microgram of Coconut Shell and It Char Samples.

4. Conclusion

1) The char properties were found to be highly dependent on the carbonization temperature. As higher temperature treatment promoted a development of more pores.
2) The increase in carbonization temperature led to the formation of char with an aromatic carbon structure and near graphitization development. Which could greatly improve electrical conductivity and reduce resistance.

Acknowledgements

References

[1] Abugu, H. O., Okoye, P. A. C.; Ajiwe, V. I. E. and Ofordile. P. C. (2014). Preparation and Characterisation of Activated Carbon from Agrowastes Peanut Seed (African Canarium) and Palm Kernel Shell. International journal of innovative research & development. 3(13), 418-441. www.ijird.com.
[2] Agu, H. O., Ukonze, J. A. and Uchola, N. O. (2008). Quality and characteristics of crude and refined Atili Oils. Pakistan journal of nutrition.7(1), 27-30. https://doi.org/10.3923/pjn.2008.27.30
[3] Bogeat, B. A. (2019): Understanding and Tuning the Electrical Conductivity of Activated Carbon: A State-of-the-Art Review, Critical Reviews in Solid State and Materials Sciences. DOI: 10.1080/10408436.2019.1671800
[4] Ding, Y., Wang, T., Dong, D. and Zhang, Y. (2020). Using biochar and coal as the electrode material for supercapacitor applications. Front. Energy Research. 7:159. doi: 10.3389/fenrg.2019.00159
[5] Ewansiha, J. C., Ebhoaye, E. J., Asia, O. I., Ekebafe, O. L. and Ehigie, C. (2012). Proximate and Mineral Composition of Coconut (*Cocos Nucifera*) Shell. International Journal of Pure Applied Science Technology. 13(1), 57-60. www.ijopaasat.in
[6] Girgis, S. B., Temerk, M. Y., Gadelrab, M. M. and Abdullah, D. I. (2007). X-ray Diffraction
[7] Hoffmann, V., Rodriguez, C. C., Sautter, D., Maringolo, E. and Kruse, A. (2019). Study of the electrical conductivity of biobased carbonaceous powder materials under moderate pressure for the application as electrode materials in energy storage technologies. GCB Bioenergy. 11:230–248.

[8]   Patterns of Activated Carbons Prepared under Various Conditions. Carbon science. 8(2), 95-100. https://doi.org/10.5714/CL.2007.8.2.095.

[9]   Kang, S. D., Lee, M. S., Lee, H. S. and Roh, S. J. (2018). X-ray diffraction analysis of the crystallinity of phenolic resin-derived carbon as a function of the heating rate during the carbonization process. Carbon Letters. 27,108-111. DOI: http://dx.doi.org/DOI:10.5714/CL.2018.27.108

[10]   Kwon, H. J., Park, B. S., Ayrilmis, N., Oh, W. S. and Kim, H. N. (2013). Effect of carbonization temperature on electrical resistivity and physical properties of wood and wood-based composites. Composites: Part B 46, 102–107. http://dx.doi.org/10.1016/j.compositesb.2012.10.012

[11]   Lee, C. L., H'ng, P. S., Paridah, T., Chin, L. K., Khoo, S. P., Nazrin, R. A. R., Asyikin, N. S. and Maminski, M. (2017). Effect of Reaction time and temperature on the properties of carbon black from palm kernel and coconut shell. Asian Journal of Scientific Research. 10(1), 24-33. https://doi.org/10.3923/ajsr.2017.24.33.

[12]   Li, W., Yanga, K., Penga, J., Zhanga, L., Guoa, S. and Xiaa, H. (2008). Effects of carbonization temperatures on characteristics of porosity in coconut shell chars and activated carbons derived from carbonized coconut shell chars. Industrial crops and products 2(8):190–198. https://doi.org/10.1016/j.indcrop.2008.02.012.

[13]   Liu, Y., He, Z. and Uchimiya, M. (2015). Comparison of Biochar Formation from Various Agricultural By-Products Using FTIR Spectroscopy. Modern Applied Science. 9(4). 246-253. https://doi.org/10.5539/mas.v9n4p246.

[14]   Liyanage D. C. and Pieris, M. (2015). A physico-chemical analysis of coconut shell powder. Procedia chemistry. 16. 222-228. www.sciencedirect.com. https://doi.org/10.1016/j.proche.2015.12.045.

[15]   Ma, X., Yuan, C. and Liu, X. (2014). Mechanical, Microstructure and Surface Characterizations of Carbon Fibers Prepared from Cellulose after Liquefying and Curing. Materials. 7:75-84. https://doi.org/10.3390/ma7010075.

[16]   Mas'udah, W. K., Astuti, F. and Darminto (2016). Study on Physical Properties of Reduced Graphene Oxide from Heating Coconut Shell. Journal of Physical Science and Engineering. 1(1). 1 – 6. http://journal2.um.ac.id/index.php/jpse. https://doi.org/10.17977/um024v1i12016p001.

[17]   Mochidzuki, K., Soutric, F., Tadokoro, K., Antal, J. M., Toth, M., Zelei, B. and Varhegyi, G. (2003). Electrical and Physical Properties of Carbonized Charcoals. Ind. Eng. Chem. Res. 42, 5140-5151.

[18]   Njeugna, E., D. Ndapeu, D., Bistac, S., Drean, Y. J., Ngenefeme J. F. and Fogue, M. (2013). Contribution to the Characterization of the Coconut Shells (Coco Nucifera) of Cameroon. International Journal of Mechanics Structural. 4(1):1-23. http://www.irphouse.com

[19]   Noh, C. H. C., Azmin, N. F. M. and Amid, A. (2017). Principal Component Analysis Application

[20]   on Flavonoids Characterization. Advances in Science, Technology and Engineering Systems Journal (2) 3, 435-440.

[21]   Ojha, S., Raghavendra, G. and Acharya, S. K. (2016). Effect of Carbonized Coconut Shell Particles on Mechanical Properties of Bio-Based Composite. Journal of Mineral Metal and Material Engineering.2:6-10. http://creativecommons.org/licenses/by-nc/3.0/. https://doi.org/10.20941/2414-2115.2016.02.2.

[22]   Olowoyo D. N. and Orere E. E (2012). Preparation and Characterization of Activated Carbon Made from Palm-Kernel Shell, Coconut Shell, Groundnut Shell and Obeche Wood (Investigation of Apparent Density, Total Ash Content, Moisture Content, Particle Size Distribution Parameters. International Journal of Research in Chemistry and Environment. 2(3),32-35. www.ijrce.org

[23]   Rampe, J. M., Setiaji, B., Trisunaryanti, W. and Triyono (2011). Fabrication and Characterization of Carbon Composite from Coconut Shell Carbon. Indonesian journal of chemistry, 11 (2):124 – 130 https://doi.org/10.22146/ijc.21398.

[24]   Reeves, J. (2012). Mid-infrared spectroscopy of biochars and spectral similarities to coal and kerogens: what are the implications? *Appl. Spectr.. 66:*689-695. https://doi.org/10.1366/11-06478.

[25]   Sanguansat, P. (ed.). (2012). *Principal component analysis - engineering applications.* Intech, Rijeka, Croatia. https://doi.org/10.5772/2693.

[26]   Satheesh, M., Pugazhvadivu, M., Prabu, B., Gunasegaran, V. and Manikandan, A. (2019). Synthesis and Characterization of Coconut Shell Ash. Journal of Nanoscience and Nanotechnology. 19. 4123–4128. www.aspbs.com/jnn. https://doi.org/10.1166/jnn.2019.16299.

[27]   Stein, I. Y., Ashley L. K., Alexander J. C., Luiz A. and Brian L. W. (2017). "Mesoscale Evolution of Non-Graphitizing Pyrolytic Carbon in Aligned Carbon Nanotube Carbon Matrix Nanocomposites." Journal of Materials Science. 52(24):13799–13811. https://doi.org/10.1007/s10853-017-1468-9.

[28]   Sulistyania, E., Tamadoa, B. D., Wulandaria, F. and Budi, E. (2015). Coconut Shell Activated Carbon as an Alternative Renewable Energy. New, Renewable Energy and Energy Conservation Conference and Exhibition. *2:76-81.* https://doi.org/10.18502/ken.v2i2.360.

[29]   Tangsathitkulchai, C., Junpirom, S. and Katesa, J. (2013). Comparison of Kinetic Models for CO_2 Gasification of Coconut-Shell Chars: Carbonization Temperature Effects on Char Reactivity and Porous Properties of Produced Activated Carbons. Engineering journal 17(1). http://www.engj.org/ https://doi.org/10.4186/ej.2013.17.1.13.

[30]   Tangsathitkulchai, C., Junpirom, S. and Katesa, J. (2016). Carbon Dioxide Adsorption in Nanopores of Coconut Shell Chars for Pore Characterization and the Analysis of Adsorption Kinetics. Journal of Nanomaterials. 2016. https://doi.org/10.1155/2016/4292316.

[31]   Wachid, M. F., Adhi Y. Perkasa, Fandi A. Prasetya, Nurul Rosyidah, and Darminto (2014). Synthesis and characterization of nanocrystalline graphite from coconut shell with heating process. AIP Conference Proceedings 1586, 202. https://doi.org/10.1063/1.4866759.

[32]   Wang, P., Zhang, J., Shao, O., Wang, G. (2018). Physicochemical properties evolution of chars from palm kernel shell pyrolysis. *Journal of Thermal Analysis and Calorimetry*. https://doi.org/10.1007/s10973-018-7185-z.